CLNS 05-1943
CLEO 05-29

New Measurements of Cabibbo-Suppressed Decays of D Mesons in CLEO-c

P. Rubin,[1] C. Cawlfield,[2] B. I. Eisenstein,[2] I. Karliner,[2] D. Kim,[2] N. Lowrey,[2] P. Naik,[2] C. Sedlack,[2] M. Selen,[2] E. J. White,[2] J. Wiss,[2] M. R. Shepherd,[3] D. Besson,[4] T. K. Pedlar,[5] D. Cronin-Hennessy,[6] K. Y. Gao,[6] D. T. Gong,[6] J. Hietala,[6] Y. Kubota,[6] T. Klein,[6] B. W. Lang,[6] R. Poling,[6] A. W. Scott,[6] A. Smith,[6] S. Dobbs,[7] Z. Metreveli,[7] K. K. Seth,[7] A. Tomaradze,[7] P. Zweber,[7] J. Ernst,[8] H. Severini,[9] S. A. Dytman,[10] W. Love,[10] S. Mehrabyan,[10] V. Savinov,[10] O. Aquines,[11] Z. Li,[11] A. Lopez,[11] H. Mendez,[11] J. Ramirez,[11] B. Xin,[12] G. S. Huang,[12] D. H. Miller,[12] V. Pavlunin,[12] B. Sanghi,[12] I. P. J. Shipsey,[12] G. S. Adams,[13] M. Anderson,[13] J. P. Cummings,[13] I. Danko,[13] J. Napolitano,[13] Q. He,[14] J. Insler,[14] H. Muramatsu,[14] C. S. Park,[14] E. H. Thorndike,[14] T. E. Coan,[15] Y. S. Gao,[15] F. Liu,[15] R. Stroynowski,[15] M. Artuso,[16] S. Blusk,[16] J. Butt,[16] J. Li,[16] N. Menaa,[16] R. Mountain,[16] S. Nisar,[16] K. Randrianarivony,[16] R. Redjimi,[16] R. Sia,[16] T. Skwarnicki,[16] S. Stone,[16] J. C. Wang,[16] K. Zhang,[16] S. E. Csorna,[17] G. Bonvicini,[18] D. Cinabro,[18] M. Dubrovin,[18] A. Lincoln,[18] D. M. Asner,[19] K. W. Edwards,[19] R. A. Briere,[20] I. Brock,[20] J. Chen,[20] T. Ferguson,[20] G. Tatishvili,[20] H. Vogel,[20] M. E. Watkins,[20] J. L. Rosner,[21] N. E. Adam,[22] J. P. Alexander,[22] K. Berkelman,[22] D. G. Cassel,[22] J. E. Duboscq,[22] K. M. Ecklund,[22] R. Ehrlich,[22] L. Fields,[22] L. Gibbons,[22] R. Gray,[22] S. W. Gray,[22] D. L. Hartill,[22] B. K. Heltsley,[22] D. Hertz,[22] C. D. Jones,[22] J. Kandaswamy,[22] D. L. Kreinick,[22] V. E. Kuznetsov,[22] H. Mahlke-Krüger,[22] T. O. Meyer,[22] P. U. E. Onyisi,[22] J. R. Patterson,[22] D. Peterson,[22] E. A. Phillips,[22] J. Pivarski,[22] D. Riley,[22] A. Ryd,[22] A. J. Sadoff,[22] H. Schwarthoff,[22] X. Shi,[22] S. Stroiney,[22] W. M. Sun,[22] T. Wilksen,[22] M. Weinberger,[22] S. B. Athar,[23] P. Avery,[23] L. Breva-Newell,[23] R. Patel,[23] V. Potlia,[23] H. Stoeck,[23] and J. Yelton[23]

(CLEO Collaboration)

[1]*George Mason University, Fairfax, Virginia 22030*
[2]*University of Illinois, Urbana-Champaign, Illinois 61801*
[3]*Indiana University, Bloomington, Indiana 47405*
[4]*University of Kansas, Lawrence, Kansas 66045*
[5]*Luther College, Decorah, Iowa 52101*
[6]*University of Minnesota, Minneapolis, Minnesota 55455*
[7]*Northwestern University, Evanston, Illinois 60208*
[8]*State University of New York at Albany, Albany, New York 12222*
[9]*University of Oklahoma, Norman, Oklahoma 73019*
[10]*University of Pittsburgh, Pittsburgh, Pennsylvania 15260*
[11]*University of Puerto Rico, Mayaguez, Puerto Rico 00681*
[12]*Purdue University, West Lafayette, Indiana 47907*
[13]*Rensselaer Polytechnic Institute, Troy, New York 12180*
[14]*University of Rochester, Rochester, New York 14627*
[15]*Southern Methodist University, Dallas, Texas 75275*
[16]*Syracuse University, Syracuse, New York 13244*
[17]*Vanderbilt University, Nashville, Tennessee 37235*
[18]*Wayne State University, Detroit, Michigan 48202*
[19]*Carleton University, Ottawa, Ontario, Canada K1S 5B6*

[20]*Carnegie Mellon University, Pittsburgh, Pennsylvania 15213*
[21]*Enrico Fermi Institute, University of Chicago, Chicago, Illinois 60637*
[22]*Cornell University, Ithaca, New York 14853*
[23]*University of Florida, Gainesville, Florida 32611*
(Dated: Dec. 22, 2005)

Abstract

Using 281 pb^{-1} of data collected with the CLEO-c detector, we report on first observations and new measurements of Cabibbo-suppressed decays of D mesons to 2, 3, 4, and 5 pions. Branching fractions of previously unobserved modes are measured to be: $\mathcal{B}(D^0 \to \pi^+\pi^-\pi^0\pi^0) = (9.9 \pm 0.6 \pm 0.7 \pm 0.2 \pm 0.1) \times 10^{-3}$, $\mathcal{B}(D^0 \to \pi^+\pi^+\pi^-\pi^-\pi^0) = (4.1 \pm 0.5 \pm 0.2 \pm 0.1 \pm 0.0) \times 10^{-3}$, $\mathcal{B}(D^+ \to \pi^+\pi^0\pi^0) = (4.8 \pm 0.3 \pm 0.3 \pm 0.2) \times 10^{-3}$, $\mathcal{B}(D^+ \to \pi^+\pi^+\pi^-\pi^0) = (11.6 \pm 0.4 \pm 0.6 \pm 0.4) \times 10^{-3}$, $\mathcal{B}(D^0 \to \eta\pi^0) = (0.62 \pm 0.14 \pm 0.05 \pm 0.01 \pm 0.01) \times 10^{-3}$, and $\mathcal{B}(D^0 \to \omega\pi^+\pi^-) = (1.7 \pm 0.5 \pm 0.2 \pm 0.0 \pm 0.0) \times 10^{-3}$. The uncertainties are from statistics, experimental systematics, normalization and CP correlations (for D^0 modes only). Improvements in other multi-pion decay modes are also presented. The $D \to \pi\pi$ rates allow us to extract the ratio of isospin amplitudes $A(\Delta I = 3/2)/A(\Delta I = 1/2) = 0.420 \pm 0.014(\mathrm{stat}) \pm 0.016(\mathrm{syst})$ and the strong phase shift of $\delta_I = (86.4 \pm 2.8 \pm 3.3)^\circ$, which is quite large and now more precisely determined.

Charm decays provide an important laboratory for the study of both the strong and weak interactions. Semileptonic decays provide direct access to CKM matrix elements. Hadronic decays provide important input to B physics as well opening a window into the study of final state (strong) interactions. Exhaustive or precise measurements of Cabibbo-suppressed decays have been challenging due to low rates or other experimental challenges, however, more information on these decays is of great importance in several areas. Firstly, in the weak sector, Cabibbo-suppressed final states, such as $D^0 \to \pi^+\pi^-\pi^0$, provide a promising way by which to extract the CKM angle γ in $B^+ \to D^{(*)0}K^{(*)}$ due to the similar magnitude of interfering amplitudes between $D^0 \to \pi^+\pi^-\pi^0$ and $\bar{D}^0 \to \pi^+\pi^-\pi^0$ [1]. In the arena of strong interactions, they provide a means in which to study final state interactions [2, 3], which may help clarify how they contribute to $B \to \pi\pi$ decay [4]. Moreover these modes can enter as backgrounds to other D decay measurements [5] and therefore their values are of general importance to ascertain. Information on these decays is sparse and not very precise. The CLEO-c $\psi(3770) \to D\bar{D}$ sample provides the opportunity to perform a comprehensive and precise study of these decays.

The CLEO-c detector is a general purpose solenoidal detector which includes a tracking system for measuring momenta and specific ionization of charged particles, a Ring Imaging Cherenkov detector to aid in particle identification, and a CsI calorimeter for detection of electromagnetic showers. The CLEO-c detector is described in detail elsewhere [6].

This analysis utilizes 281 pb^{-1} of data collected on the $\psi(3770)$ resonance ($\sqrt{s} \approx 3.77$ GeV) at the Cornell Electron Storage Ring. At this energy, $D\bar{D}$ pairs are produced in a coherent 1^{--} final state with no additional particles.

We reconstruct D^0 mesons in several multi-pion decay channels, including $D^0 \to \pi^+\pi^-$, $D^0 \to \pi^0\pi^0$, $D^0 \to \pi^+\pi^-\pi^0$, $D^0 \to \pi^+\pi^+\pi^-\pi^-$, $D^0 \to \pi^+\pi^-\pi^0\pi^0$, $D^0 \to \pi^+\pi^+\pi^-\pi^-\pi^0$ and $D^0 \to \pi^0\pi^0\pi^0$. In D^+ we reconstruct $D^+ \to \pi^+\pi^0$, $D^+ \to \pi^+\pi^+\pi^-$, $D^+ \to \pi^+\pi^0\pi^0$, $D^+ \to \pi^+\pi^+\pi^-\pi^0$, $D^+ \to \pi^+\pi^+\pi^+\pi^-\pi^-$. We also consider the resonant η and ω contributions and measure rates for $D^0 \to \eta\pi^0$, $D^0 \to \omega\pi^+\pi^-$, and $D^+ \to \eta\pi^+$. The branching fractions are measured relative to $D^0 \to K^-\pi^+$ and $D^+ \to K^-\pi^+\pi^+$ for neutral and charged D mesons, respectively. Throughout the paper, charge conjugate modes are implicitly assumed, unless otherwise noted.

The reconstruction of D mesons uses charged particles and π^0's reconstructed with standard selection requirements [7]. For each candidate, we utilize two kinematic variables: $\Delta E = E_{\rm beam} - E_D$ and $M_{\rm bc} = \sqrt{E^2_{\rm beam} - p^2_D}$, where E_D (p_D) are the energy (momentum) of the D candidate and $E_{\rm beam}$ is the beam energy. The substitution of the beam energy for the candidate energy improves the mass resolution by about a factor of five. For properly reconstructed candidates, ΔE exhibits a narrow peak near zero and $M_{\rm bc}$ peaks at the D meson mass. Mode-dependent signal regions in ΔE are defined to be within about three times the r.m.s. widths of the ΔE distribution obtained from detailed Monte Carlo (MC) simulations (see Table I). A ΔE sideband region extending from 10 MeV beyond the signal region to 100 MeV is used to study the shape of the background in $M_{\rm bc}$.

The Cabibbo-favored modes such as $D \to K^0_S + X$, $K^0_S \to \pi\pi$ constitute a large background as their branching fractions are typically five to ten times larger than the Cabibbo-suppressed modes, and therefore such events must be vetoed. For each decay channel with $\geq$ three pions, we veto any candidate which contains a pair of pions with invariant mass in the range $475 < M_{\pi^+\pi^-} < 520$ MeV/c^2 or $448 < M_{\pi^0\pi^0} < 548$ MeV/c^2. This range was determined from a large sample of generic MC events where we require that the surviving K^0_S background be less than 1% of the expected signal in the corresponding Cabibbo-suppressed

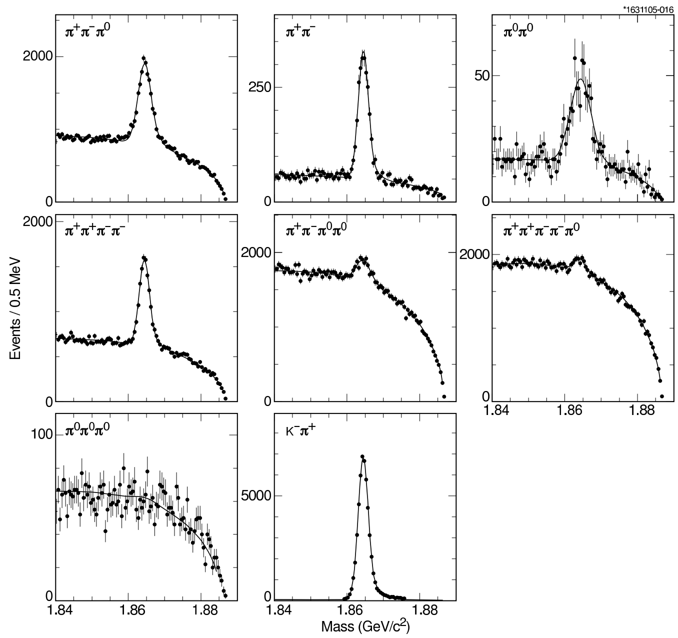

FIG. 1: $M_{\rm bc}$ distributions for D^0 modes from data. The points are the data and the superimposed lines are the fits as described in the text.

signal channel.

The resulting $M_{\rm bc}$ distributions for the neutral and charged D modes are shown in Figs. 1 and 2, respectively. The points show the data from the ΔE signal region and the lines are fits to the distributions which are given by the sum of an ARGUS threshold function [8] and an asymmetric signal shape(CBAL) [9] which models the initial state radiation (ISR) induced tail at large $M_{\rm bc}$. The ARGUS shape parameters are extracted by fitting the ΔE sidebands. The signal shape parameters are determined by fits to $M_{\rm bc}$ distributions obtained from a simulation of $D\bar{D}$ production at the $\psi(3770)$ [10] followed by a simulation of the detector response [11, 12]. The Gaussian widths of the $M_{\rm bc}$ distributions, which are part of the CBAL signal shape, and the fitted yields are listed in Table I. The yields we find for the normalization modes are in good agreement with the previously published values [7].

Efficiencies for a given decay mode depend mildly on the presence of intermediate resonances, but the dependence is increased to as large as 10% (relative) when the K_S^0 veto is included. To minimize this bias, we tune the MC simulation by either using existing Dalitz-plot analyses, as for the $\pi\pi\pi$ final states [13, 14], or by adding intermediate resonances to each mode in order to reproduce the observed substructure in the $\pi\pi$ invariant mass distribution. In most cases, this requires introducing significant ρ contributions. Efficiencies from simulation are checked in data by comparing the numbers of particles of each species in fully reconstructed events with the corresponding yields when their populations are inferred from energy and momentum conservation [7]. The resulting corrections are: (-3.9$\pm$2.0)% per π^0, (-0.7$\pm$0.7)% per $K^\pm$ and (-0.3$\pm$0.3)% per $\pi^\pm$ [7]. For π^0's with momentum near $M_D/2$, the correction is (-4.6 ± 3.5)%. The resulting efficiencies are shown in the last column of Table I.

These multi-pion final states are fed by intermediate resonances, such as ρ, η, ω, ϕ, f_0, f_2, etc. We examine the multipion final states for η, $\omega \to \pi^+\pi^-\pi^0$ only. The $\phi \to \pi^+\pi^-\pi^0$

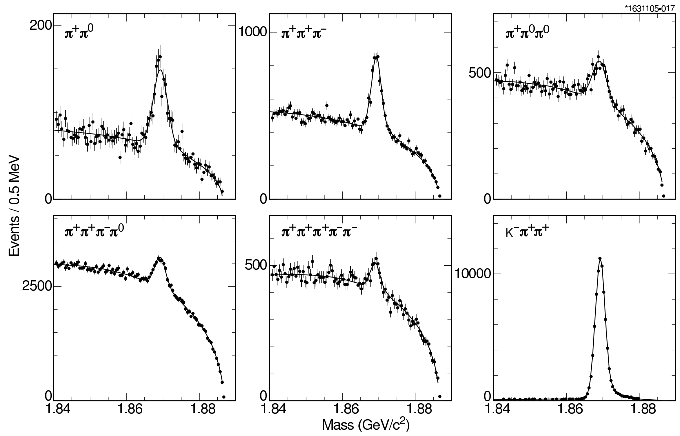

FIG. 2: $M_{\rm bc}$ distributions for D^+ modes from data. The points are the data and the superimposed lines are the fits as described in the text.

TABLE I: Requirements on ΔE for signal candidates, Gaussian widths of the $M_{\rm bc}$ distributions, observed yields, and reconstruction efficiencies. See text for details.

Mode	ΔE [low, high] (MeV)	$M_{\rm bc}$ Width (MeV)	Yield	Efficiency (%)
$D^0 \to \pi^+\pi^-$	[-30, 30]	1.42	2085±54	73.1±0.7
$D^0 \to \pi^0\pi^0$	[-50, 40]	2.88	499±32	31.0±0.7
$D^0 \to \pi^+\pi^-\pi^0$	[-50, 40]	1.83	10834±164	39.9±0.7
$D^0 \to \pi^+\pi^+\pi^-\pi^-$	[-25, 25]	1.46	7331±130	48.4±0.6
$D^0 \to \pi^+\pi^-\pi^0\pi^0$	[-40, 30]	2.02	2724±166	15.9±0.5
$D^0 \to \pi^+\pi^+\pi^-\pi^-\pi^0$	[-30, 20]	1.67	1614±171	18.4±0.6
$D^0 \to \pi^0\pi^0\pi^0$	[-60, 35]	3.00	29±15	13.4±0.7
$D^0 \to K^-\pi^+$	[-29, 29]	1.42	51210±231	65.0±0.6
$D^+ \to \pi^+\pi^0$	[-40, 35]	1.98	914±46	46.5±0.8
$D^+ \to \pi^+\pi^+\pi^-$	[-25, 25]	1.40	3303±95	62.0±0.8
$D^+ \to \pi^+\pi^0\pi^0$	[-30, 30]	1.99	1535±89	22.0±0.6
$D^+ \to \pi^+\pi^+\pi^-\pi^0$	[-30, 30]	1.58	5701±205	30.6±0.7
$D^+ \to \pi^+\pi^+\pi^+\pi^-\pi^-$	[-15, 15]	1.38	732±77	27.6±0.6
$D^+ \to K^-\pi^+\pi^+$	[-22, 22]	1.37	80381±290	54.4±0.5

intermediate state is not treated here since it can be measured significantly better using $\phi \to K^+K^-$, and the observed rates are too low to improve on existing measurements.

We search the $D^+ \to \pi^+\pi^+\pi^-\pi^0$, $D^0 \to \pi^+\pi^-\pi^0\pi^0$, and $D^0 \to \pi^+\pi^+\pi^-\pi^-\pi^0$ modes for η and ω decays. The yields are extracted by selecting events that are within 2.5 times the r.m.s. width of the D mass and taking the difference in yields between the number of such events in the ΔE signal and ΔE sideband regions. The sideband distributions are normalized to account for the different range of ΔE between signal and sidebands regions. Distributions of $\pi^+\pi^-\pi^0$ mass for these three modes are shown in Fig. 3. The left column shows combinations whose ΔE is in the signal region and the right column shows candidates in the ΔE sideband

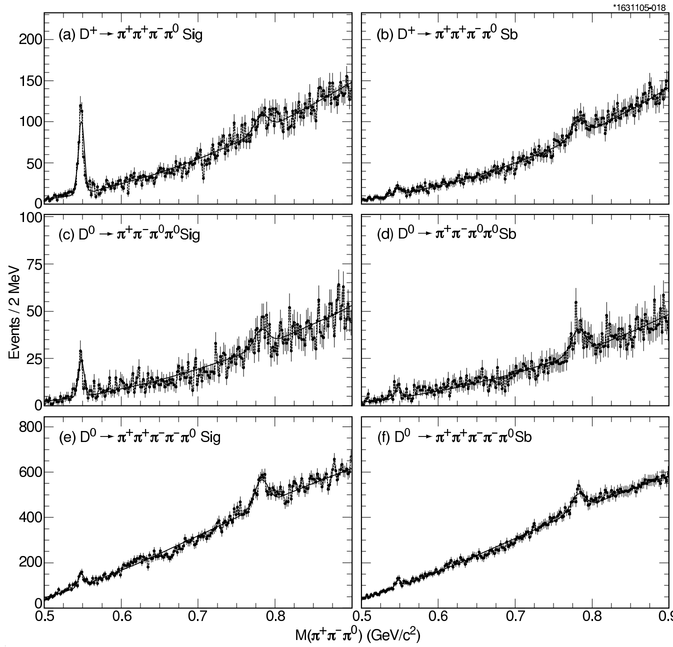

FIG. 3: Distributions in $\pi^+\pi^-\pi^0$ invariant mass for $D^+ \to \pi^+\pi^+\pi^-\pi^0$ (a,b), $D^0 \to \pi^+\pi^-\pi^0\pi^0$ (c,d), and $D^0 \to \pi^+\pi^+\pi^-\pi^-\pi^0$ (e,f) candidates. The left column represents the ΔE signal region and the right are for ΔE sidebands. The superimposed lines are the fits as described in the text.

region. The distributions are fit to the sum of a polynomial background and two Gaussians, one each for the η and ω. With the limited statistics and large background, we do not try to fit the Breit-Wigner tails of the ω, but rather assume a Gaussian shape and absorb the loss of events from the tails into the efficiency. In the fit, the η and ω Gaussian widths are constrained to 3.8 MeV and 9.0 MeV, respectively, the values determined from signal MC. The resulting yields for the ΔE signal and sideband regions are shown in Table II along with the reconstruction efficiency, determined from signal MC.

TABLE II: Summary of submodes containing η and ω mesons, indicating efficiencies and yields in the ΔE signal and ΔE sideband regions.

Mode	Efficiency (%)	Yield ΔE signal	Yield ΔE sideband
$D^+ \to \eta\pi^+$	29.4±1.0	421±23	44±12
$D^+ \to \omega\pi^+$	21.7±1.0	216±43	236±41
$D^0 \to \eta\pi^0$	21.9±1.0	90±12	28±8
$D^0 \to \omega\pi^0$	14.1±1.0	103±26	140±25
$D^0 \to \eta\pi^+\pi^-$	20.3±1.0	260±32	150±29
$D^0 \to \omega\pi^+\pi^-$	15.6±1.1	1304±96	832±91

Relative branching fractions are computed using the yields shown in Tables I and II and are presented in Table III (unseen decay modes of the η and ω are included, using $\mathcal{B}(\eta,\omega \to \pi^+\pi^-\pi^0)$ from Ref. [15]). To compute the absolute branching fractions, we use $\mathcal{B}(D^0 \to K^-\pi^+) = (3.84\pm0.07)\%$ and $\mathcal{B}(D^+ \to K^-\pi^+\pi^+) = (9.4\pm0.3)\%$, which are obtained

using a weighted average of the PDG values and the recent CLEO measurements [7]. For unobserved modes, we set 90% confidence level upper limits. In the last column of Table III we show PDG [15] averages, when available.

TABLE III: Measured relative and absolute branching fractions for neutral and charged D modes. Uncertainties are statistical, experimental systematic, normalization mode uncertainty, and uncertainty from CP correlations (for D^0 modes only). For the relative branching fractions, the normalization mode uncertainty is omitted.

Mode	$\mathcal{B}_{\rm mode}/\mathcal{B}_{\rm ref}$ (%)	$\mathcal{B}_{\rm mode}$ (10^{-3})	$\mathcal{B}$ (PDG) (10^{-3})
$D^0 \to \pi^+\pi^-$	$3.62 \pm 0.10 \pm 0.07 \pm 0.04$	$1.39 \pm 0.04 \pm 0.04 \pm 0.03 \pm 0.01$	1.38±0.05
$D^0 \to \pi^0\pi^0$	$2.05 \pm 0.13 \pm 0.16 \pm 0.02$	$0.79 \pm 0.05 \pm 0.06 \pm 0.01 \pm 0.01$	0.84±0.22
$D^0 \to \pi^+\pi^-\pi^0$	$34.4 \pm 0.5 \pm 1.2 \pm 0.3$	$13.2 \pm 0.2 \pm 0.5 \pm 0.2 \pm 0.1$	11±4
$D^0 \to \pi^+\pi^+\pi^-\pi^-$	$19.1 \pm 0.4 \pm 0.6 \pm 0.2$	$7.3 \pm 0.1 \pm 0.3 \pm 0.1 \pm 0.1$	7.3±0.5
$D^0 \to \pi^+\pi^-\pi^0\pi^0$	$25.8 \pm 1.5 \pm 1.8 \pm 0.3$	$9.9 \pm 0.6 \pm 0.7 \pm 0.2 \pm 0.1$	
$D^0 \to \pi^+\pi^+\pi^-\pi^-\pi^0$	$10.7 \pm 1.2 \pm 0.5 \pm 0.1$	$4.1 \pm 0.5 \pm 0.2 \pm 0.1 \pm 0.0$	
$D^0 \to \omega\pi^+\pi^-$	$4.1 \pm 1.2 \pm 0.4 \pm 0.0$	$1.7 \pm 0.5 \pm 0.2 \pm 0.0 \pm 0.0$	
$D^0 \to \eta\pi^0$	$1.47 \pm 0.34 \pm 0.11 \pm 0.01$	$0.62 \pm 0.14 \pm 0.05 \pm 0.01 \pm 0.01$	
$D^0 \to \pi^0\pi^0\pi^0$	-	< 0.35 (90% CL)	
$D^0 \to \omega\pi^0$	-	< 0.26 (90% CL)	
$D^0 \to \eta\pi^+\pi^-$	-	< 1.9 (90% CL)	
$D^+ \to \pi^+\pi^0$	1.33±0.07±0.06	1.25±0.06±0.07±0.04	1.33±0.22
$D^+ \to \pi^+\pi^+\pi^-$	3.52±0.11±0.12	3.35±0.10±0.16±0.12	3.1±0.4
$D^+ \to \pi^+\pi^0\pi^0$	5.0±0.3±0.3	4.8±0.3±0.3±0.2	
$D^+ \to \pi^+\pi^+\pi^-\pi^0$	12.4±0.5±0.6	11.6±0.4±0.6±0.4	
$D^+ \to \pi^+\pi^+\pi^+\pi^-\pi^-$	1.73±0.20±0.17	1.60±0.18±0.16±0.06	1.73±0.23
$D^+ \to \eta\pi^+$	3.81±0.26±0.21	3.61±0.25±0.23±0.12	3.0±0.6
$D^+ \to \omega\pi^+$	-	< 0.34 (90% CL)	

Several sources of systematic uncertainty are considered. Where appropriate, we include in parentheses the minimum to maximum size of the uncertainty. Limited MC statistics are used in determining the reconstruction efficiencies, which introduce relative uncertainties at the level of (1-3)%. Tracking and π^0 reconstruction efficiencies have relative uncertainties of 0.7% and 2.0% (3.5% for high momentum π^0) per particle, respectively, and charged particle identification is understood at the level $0.3\%/\pi^\pm$ and $1.3\%/K^\pm$. Uncertainty from the K^0_S veto is estimated as the difference in probabilities (between data and MC) for each final state to pass the K^0_S veto. This survival fraction, $F^{\pi\pi}$, is given by $F^{\pi\pi} \equiv (1 - f_{\rm veto})^{N_{\rm pair}}$, where $f_{\rm veto}$ represents the veto probability per $\pi\pi$ pair, which is obtained by a linear interpolation from an 80 MeV region above and below the veto region, and $N_{\rm pair}$ is the number of $\pi^+\pi^-$ (or $\pi^0\pi^0$) pairs in the given decay mode. The uncertainties on the veto efficiencies for $\pi^+\pi^-$ and $\pi^0\pi^0$ are added in quadrature when applicable (0.0%-2.8%). Uncertainties in signal yields are estimated by comparing changes in the branching fraction when (a) signal widths are permitted to float, (b) varying the ISR-tail shape parameters individually by ±1 standard deviation, and (c) varying the range of the fit to the $M_{\rm bc}$ distribution. The three sources are

added in quadrature to obtain the total uncertainties (1.0%-4.9%). Uncertainties resulting from different ΔE resolutions are quantified by widening the ΔE windows, recomputing the branching fractions, and taking the difference between the new and default values (0.2%-7.7%). The simulation of final state radiation has been studied in $J/\psi \to \mu^+\mu^-$ events and is estimated to introduce no more than 0.5% uncertainty on the D reconstruction efficiency. Possible bias due to resonant substructure is estimated by removing the K_S^0 veto (so as not to double count this systematic) and comparing the efficiencies obtained using our default simulation (which includes resonances) and a phase space simulation (0.0%-2.2%). Imperfect replication of the average number of candidates per event by the simulation could lead to a bias in the reconstruction efficiency. This effect is quantified by comparing the average number of D candidates per event, $\langle N_{\rm cand}\rangle$, within 2.5 standard deviations of the D mass, between data and simulation (on a mode-by-mode basis). The systematic uncertainty is taken as the difference in the ratio from unity, *i.e.,* $\langle N_{\rm cand}^{\rm data}\rangle/\langle N_{\rm cand}^{\rm MC}\rangle - 1$ (0.2%-2.7%). The D^0 and D^+ normalization modes introduce uncertainties of 1.8% and 3.2%, respectively. Lastly, the effects of quantum correlations of $D\bar{D}$ pairs produced from the 1^{--} $\psi(3770)$ may shift the branching fractions with respect to the values in the absence of these correlations. The effect of these quantum correlations has been considered [16], and a shift in the branching fraction can be expected if $y = \Delta\Gamma/\Gamma \neq 0$. Limits on y are at the percent level [15], and we take this as an additional systematic uncertainty on the D^0 branching fractions. The total systematic uncertainties on the branching fractions for each mode are shown in Table III.

Using the new $D \to \pi\pi$ branching fractions and D lifetimes, $\tau_{D^+} = (1040 \pm 7)$ fs and $\tau_{D^0} = (410.3 \pm 1.5)$ fs [15], we compute the ratio of the $\Delta I = 3/2$ to $\Delta I = 1/2$ isospin amplitudes and their relative strong phase difference [17] to be $A_2/A_0 = 0.420 \pm 0.014(\text{stat}) \pm 0.01(\text{syst})$ and $\cos\delta_I = 0.062 \pm 0.048(\text{stat}) \pm 0.058(\text{syst})$. The large phase shift, $\delta_I = (86.4 \pm 2.8 \pm 3.3)^\circ$, indicates that final state interactions are important in $D \to \pi\pi$ transitions. These results represent a considerable improvement over previous measurements from CLEO [18] and FOCUS [19], both of which are consistent with our data.

In summary, we report new measurements of six Cabibbo-suppressed decay branching fractions of D mesons and eight additional measurements, of which all except for $D^0 \to \pi^+\pi^-$ and $D^+ \to \pi^+\pi^+\pi^+\pi^-\pi^-$ provide large improvements over the existing world average values. The large value of the strong phase shift, δ_I obtained in the $D \to \pi\pi$ decay supports the conclusion that final state interactions are important in D decays.

We gratefully acknowledge the effort of the CESR staff in providing us with excellent luminosity and running conditions. This work was supported by the A.P. Sloan Foundation, the National Science Foundation, and the U.S. Department of Energy.

[1] B. Aubert *et al.* (BaBar Collaboration), hep-ex/0505084.

[2] X. Wu *et al.,* Mod. Phys. Lett. **A19**, 1623 (2004).

[3] M. Ablikim, D. Du, and M. Yang, Phys. Lett. B **536**, 34 (2002).

[4] P. Guo, X. He, and X. Li, hep-ph/0402262, and references therein.

[5] For example, $D^+ \to \pi^+\pi^0$ is a background to $D^+ \to \mu^+\nu_\nu$, $D^+ \to \pi^+\pi^0\pi^0$ is a background to the inclusive $D^+ \to K^0\pi^+$ analysis.

[6] D. Peterson *et al.,* Nucl. Instrum. Meth. A**478**, 142 (2002); M. Artuso *et al.,* Nucl. Instrum. Meth. A**554**, 147 (2005); Y. Kubota *et al.,* Nucl. Instrum. Meth. A**320**, 66 (1992).

[7] Q. He *et al.* (CLEO Collaboration), Phys. Rev. Lett. **95**, 121801 (2005).

[8] H. Albrecht *et al.* (ARGUS Collaboration) Phys. Lett. B**229**, 304 (1989).
[9] T. Skwarnicki, "A Study of the Radiative Cascade Transitions between Υ' and Υ Resonances", DESY F31-86-02, (thesis, unpublished) (1986).
[10] D. J. Lange, Nucl. Instrum. Meth. Phys. Res. Sec. A **462**, 152 (2001).
[11] R. Brun *et al.,* GEANT 3.21, CERN Program Library Long Writeup W5013 (unpublished), 1993.
[12] E. Barberio and Z. Was, Comput. Phys. Commun. **79**, 291 (1994).
[13] D. Cronin-Hennessey *et al.* (CLEO Collaboration), Phys. Rev. D**72**, 031102 (2005).
[14] E. M. Aitala *et al.* (E791 Collaboration) Phys. Rev. Lett. **86**, 770 (2001).
[15] S. Eidelman *et al.,* Phys. Lett. B**592**, 1 (2004) and 2005 partial update for the 2006 edition available on the PDG WWW pages (URL: http://pdg.lbl.gov/) .
[16] D. Asner and W. Sun (submitted to Phys. Rev. D); [hep-ph/0507238].
[17] M. Selen *et al.* (CLEO Collaboration), Phys. Rev. Lett. **71**, 1973 (1993).
[18] K. Arms *et al.* (CLEO Collaboration), Phys. Rev. D**69**, 071102 (2004).
[19] J. M. Link *et al.* (FOCUS Collaboration), Phys. Lett. B**555**, 167 (2003).